Neuron, Vol. 21, 813–825, October, 1998, Copyright ©1998 by Cell Press

Tissue Plasminogen Activator Contributes to the Late Phase of LTP and to Synaptic Growth in the Hippocampal Mossy Fiber Pathway

Danny Baranes,*†§ Doron Lederfein,*†‖
Yan-You Huang,† Mary Chen,†
Craig H. Bailey,† and Eric R. Kandel*†‡
*Howard Hughes Medical Institute and
†Center for Neurobiology and Behavior
College of Physicians and Surgeons
Columbia University
New York, New York 10032

Summary

The expression of tissue plasminogen activator (tPA) is increased during activity-dependent forms of synaptic plasticity. We have found that inhibitors of tPA inhibit the late phase of long-term potentiation (L-LTP) induced by either forskolin or tetanic stimulation in the hippocampal mossy fiber and Schaffer collateral pathways. Moreover, application of tPA enhances L-LTP induced by a single tetanus. Exposure of granule cells in culture to forskolin results in secretion of tPA, elongation of mossy fiber axons, and formation of new, active presynaptic varicosities contiguous to dendritic clusters of the glutamate receptor R1. These structural changes are blocked by tPA inhibitors and induced by application of tPA. Thus, tPA may be critically involved in the production of L-LTP and specifically in synaptic growth.

Introduction

In higher invertebrates and perhaps vertebrates as well, memory storage is accompanied by alterations in the structure of synaptic connections (for review, Bailey and Kandel, 1993). Rapid and transient modifications of the synapse, as are thought to be involved in short-term memory processes, are thought to affect synaptic efficacy through alterations in the location of vesicles in relation to their site of release or in the activity of synaptic vesicle–associated proteins. By contrast, more enduring synaptic changes involved in long-term memory appear to require a more pronounced modification of neuronal architecture, such as changes in the number or pattern of synaptic connections. For example, behavioral memory for long-term sensitization in *Aplysia*, both in the intact animal (Bailey and Chen, 1988, 1989) and in dissociated cell culture (Glanzman et al., 1990; Bailey et al., 1992), is accompanied by major structural changes that include an enduring increase in the number of synapses which the sensory neurons make on their target cells, the interneurons, and motor neurons. Formation of new synapses has also been found following long-term potentiation (LTP) in the mammalian hippocampus (Lee et al., 1980; Chang and Greenough, 1984; Geinisman et al., 1991, 1993) or following epileptic seizures (Nitecka et al., 1984; Tauck and Nadler, 1985; Okazaki and Nadler, 1988). Moreover, although Sorra and Harris (1998) have reported that synaptic number and size are stable 2 hr after LTP in the CA1 region, recent biophysical analyses suggest that the late phase of LTP (L-LTP) in the Schaffer collateral pathway may be associated with an increase in the number of synaptic release sites (Bolshakov et al., 1997).

These findings indicate that long-term memory storage is accompanied by structural changes in the participating neurons and raise the question, what molecules contribute to the cellular cascade that converts electrical signals into the formation of new and persistent synaptic connections? One attractive candidate is tissue plasminogen activator (tPA), a plasma serine protease that has as one of its functions conversion of plasminogen to plasmin, leading to the degradation of blood clots (Mayer, 1990).

Although tPA is expressed in the CNS, its role there is not known. Since it is secreted by neurons during neurite outgrowth and tissue remodeling (Monard, 1988; Pittman et al., 1989; Seeds et al., 1990; Sumi et al., 1992; Griesinger and Müller, 1996, Soc. Neurosci., abstract), tPA has been thought to be an important regulatory molecule in neuronal development and in the modulation of neuronal architecture and neuronal death (Tsirka et al., 1996). The most common idea is that tPA acts to degrade the extracellular matrix, facilitating axon elongation. Several potential substrates of tPA are thought to participate in this process, including the cell adhesion molecule fibronectin (Seeds et al., 1990), the hepatocyte growth factor (HGF) (Naldini et al., 1995; Thewke and Seeds, 1996), and plasminogen (Tsirka et al., 1997). For example, HGF, a plasminogen-like protein is activated by tPA and induces morphogenesis and invasive growth of epithelial and endothelial cells, by activating its tyrosine kinase receptor, c-Met (Bottaro et al., 1991; Rosen et al., 1994; Ebens et al., 1996). Plasminogen, produced in the hippocampus (Tsirka et al., 1997), similarly is a physiological, neuronal substrate for tPA in the brain. For example, tPA-null mice and plasminogen-null mice are both resistant to neuronal degradation, and inhibitors of tPA and inhibitors of plasmin can block kainate-induced death.

Several lines of evidence suggest that tPA activity might be important for learning-related synaptic plasticity. First, tPA mRNA expression is induced by LTP (Qian et al., 1993). Second, an increased level of tPA protein is found in the cerebellum after motor learning training (Seeds et al., 1995). Finally, mice that lack the gene encoding tPA show a selective defect in L-LTP (Frey et al., 1996; Huang et al., 1996). These animals also have a defect in spatial learning (Hans-Peter Lipp, personal communication).

To examine the possible role played by tPA in LTP and in synapse formation, we have utilized two different experimental systems. First, we studied the actions of

‡To whom correspondence should be addressed (e-mail: erk5@columbia.edu).
§Present address: Department of Anatomy and Cell Biology, McGill University, Montreal, Quebec, Canada.
‖Present address: Montreal Neurological Institute, McGill University, Montreal, Quebec, Canada.

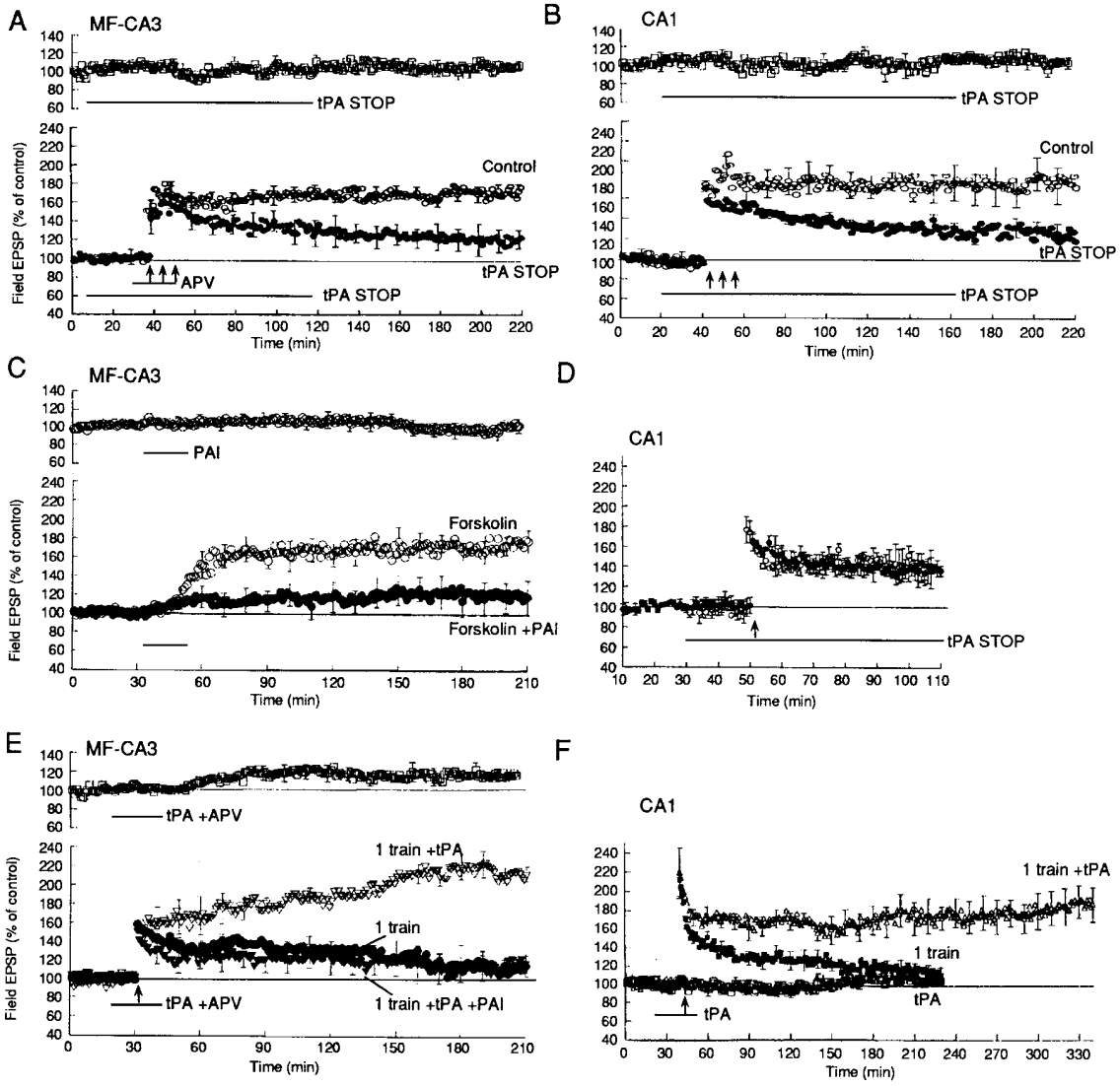

Figure 1. Inhibitors of tPA Block L-LTP

(A) tPA stop selectively blocked L-LTP induced by three tetani (100 Hz, 1 s) in the mossy fiber CA3 pathway. tPA stop was perfused for 30 min before tetanus and maintained for 2 hr after tetanus. In the presence of tPA stop, L-LTP was depressed. APV was present for 20 min, starting 10 min before the stimulation. Open circles, control; filled circles, tPA stop. tPA stop has no effect on baseline field EPSPs (top panel).

(B) In the presence of tPA stop (2 μM), LTP in the Schaffer collateral pathway induced by three trains of tetanus (100 Hz, 1 s) was significantly depressed (filled circles). Open circles, control. tPA stop (2 μM) has no effect on baseline field EPSPs (top panel).

(C) A brief application of forskolin (50 μM) induced a long-lasting potentiation in mossy fiber–CA3 pathway (open circles), this potentiation was inhibited by tPA inhibitor PAI-1 (1 μg/ml) (filled circles). PAI-1 has no effect on the baseline field EPSP (top panel).

(D) tPA stop has no effect on the early phase of LTP induced by a single train of tetanus (100 Hz, 1 s). Open circles, control; filled circles, tPA stop.

(E) When the application of tPA (0.5 μg/ml) was paired with a single tetanus (100 Hz, 1 s), L-LTP was induced in mossy fiber–CA3 pathway (open triangles). LTP induced by a single tetanus alone decayed to baseline (filled circles). The facilitated induction of L-LTP by tPA was inhibited by the tPA inhibitor PAI-1 (filled triangles). Perfusion of tPA alone without pairing of tetanus induced only slight synaptic potentiation in this pathway (top panel). APV was present for 20 min, starting 10 min before the stimulation.

(F) When the application of tPA was paired with a single train of tetanus, a sustained L-LTP was induced (open triangles) in the Schaffer collateral pathway. LTP induced by a single train alone decayed to baseline within 3 hr (filled squares). TPA alone has no effect on the baseline field EPSPs (open squares).

tPA physiologically, in hippocampal slices where we examined both the mossy fiber and the Schaffer collateral pathways. Second, we studied the role of tPA in synapse formation, using a dissociated cell culture system that allowed us to examine individual mossy fibers and their synaptic connections (Baranes et al., 1996; López-García et al., 1996).

As in the earlier genetic studies (Frey et al., 1996; Huang et al., 1996), our results in hippocampal slices indicate that L-LTP in the mossy fiber pathway induced by either tetanic stimulation or forskolin can be blocked selectively by inhibitors of tPA. In culture, we find that forskolin stimulation leads to elongation of mossy fiber axons and formation of new synaptic connections. Both

axonal elongation and formation of new synaptic connections are blocked by inhibitors of tPA. Thus, we demonstrate that the extracellular activity of the serine protease tPA contributes to L-LTP in slices and stimulates synapse formation in culture.

Results

tPA Inhibitor Blocks L-LTP

Qian et al. (1993) first showed that repeated tetani that induce LTP lead to an induction of tPA mRNA. More recently, Huang et al. (1996) and Frey et al. (1996) found that mice, in which the tPA gene has been ablated, show a selective reduction in hippocampal L-LTP, both in the Schaffer collateral–CA1 and mossy fiber–CA3 pathways. Together these results provided the initial evidence that tPA is involved in L-LTP.

To further examine the role of tPA in LTP, we next tested the effect of the tPA inhibitor, tPA stop. Since the induction of L-LTP requires transcription during a critical window of time (Nguyen et al., 1994), and the increase in tPA mRNA following LTP lasts for several hours after tetanus (Qian et al., 1993), we perfused the tPA inhibitor (2 μM) for 30 min before tetanus and maintained perfusion for 90 min after tetanus. The tPA inhibitor, tPA stop, selectively depressed the late and the intermediate phases of LTP induced by three trains of tetanization (Huang and Kandel, 1994), in both the mossy fiber (Figure 1A) and the Schaffer collateral (Figure 1B) pathways. In the mossy fiber pathway, LTP was significantly decreased in the presence of tPA stop 3 hr after tetanus, when compared to control preparations (+ tPA stop 120% $\pm$ 10%, control 168% $\pm$ 6%, $n = 6$, $p < 0.01$; Figure 1A). Similarly, in the Schaffer collateral pathway, LTP in the presence of tPA stop was 118% $\pm$ 3% 3 hr after tetanus, compared to control (170% $\pm$ 18%, $n = 5$, $p < 0.01$; Figure 1B). tPA stop had no effect on the baseline EPSP in either the Schaffer collateral pathway or the mossy fiber pathway (upper panels, Figures 1A and 1B).

Consistent with earlier physiological results, we found that the tPA stop had no effect on the early phase of LTP induced by a single tetanus (Figure 1D), suggesting that inhibition of tPA selectively blocked the protein synthesis–dependent L-LTP without affecting the LTP induction mechanism (Huang et al., 1994). By contrast, application of tPA stop 10–60 min following the tetanus had no effect on mossy fiber LTP ($n = 2$, data not shown). This suggests that tPA is either a component of the mechanism that induces L-LTP or is involved in its maintenance by affecting the activity of proteins synthesized immediately after tetanic stimulation.

Brief application of forskolin, an activator of adenylate cyclase, also induces a protein synthesis–dependent L-LTP that has the properties of the L-LTP induced by repeated tetani (Huang et al., 1996). To test whether forskolin-induced potentiation is mediated by endogenous tPA, we examined the effect of the tPA inhibitor, plasminogen activator inhibitor (PAI-1). In the presence of PAI-1 (1 μg/ml), forskolin-induced potentiation was significantly reduced at 3 hr (+PAI-1 121% $\pm$ 18%, $n = 4$) when compared to controls (178% $\pm$ 12%, $n = 4$, $p < 0.05$) (Figure 1C). This result is consistent with findings that forskolin-induced potentiation is depressed in mice in which the tPA gene has been knocked out (Huang et al., 1996) and suggests that transcription of the tPA gene is presumably downstream from CREB and the cAMP-PKA cascade. Consistent with this idea, the tPA promoter contains a cAMP-responsive element (CRE) (Ohlsson et al., 1993).

To test whether tPA can facilitate the induction of

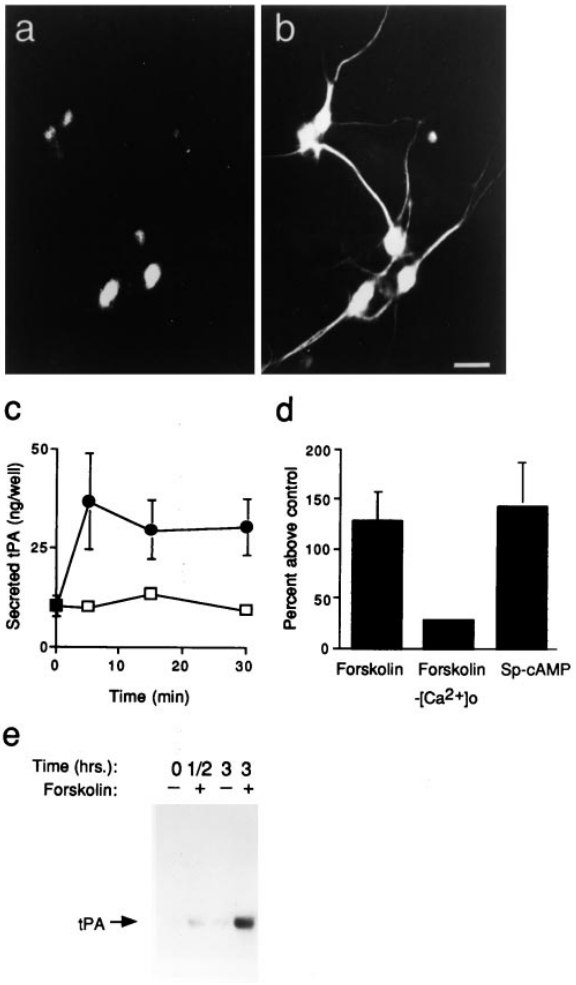

Figure 2. tPA Is Present in Neurons and Is Released by Forskolin Stimulation

(a) tPA immunoreactivity is concentrated in neuronal cell bodies.

(b) The same field as (a) stained with antibodies against MAP2. Note colocalization of tPA and MAP2 immunoreactivity in neuronal somata. Scale bar, 30 μm.

(c) Kinetics of tPA release. Two-week-old cells were exposed to forskolin (filled circles) or control solution (open squares) for different time intervals. The supernatant was collected and analyzed by ELISA for content of tPA. Shown is the mean $\pm$ SEM of five separate experiments. Error bars of the control are smaller than the data point symbols.

(d) In three separate experiments, release of tPA was measured 5 min after forskolin treatment in the absence of extracellular Ca^{2+} or after stimulation with Sp-cAMP. Shown is the mean $\pm$ SEM. The SEM of the middle bar is close to zero.

(e) Northern blot showing tPA mRNA expression in forskolin stimulated (+) and control (−) cells. Shown are RNA samples (5 μg/lane) of one representative experiment out of three. The blot was probed with mouse tPA cDNA (Rickles et al., 1988) and β-actin cDNA to control for the amount of RNA loaded (data not shown).

Table 1. Quantitative Spatial Relationship between Varicosity Formation, Presynaptic Accumulation of Recycled Vesicles, and Clustering of Postsynaptic GluR1 Receptors

Components of DiI$^+$ Synaptic Connection	DiI$^+$ Varicosities (%)	Synaptophysin$^+$ Varicosities (%)	FM-143 Secreting Varicosities (%)
Synaptophysin$^+$ varicosity	83.2 ± 1.4		
FM-143 secretion	64.1 ± 8.6	77.0 ± 10.3	
GluR1 cluster	88.5 ± 11.5	95.0 ± 4.6	100
Synaptophysin$^+$ varicosity and GluR1 cluster	79.0 ± 1.3		
FM-143 secretion and GluR1 cluster	64.1 ± 8.6		
Synaptophysin$^-$ varicosity and GluR1 cluster$^+$	4.3 ± 1.3		

At the termination of the experiment, fluorescent images of FM-143, synaptophysin, and GluR1 antibodies were collected from the same field and digitally assigned different colors. Superimposition of the resultant images yielded a new color only at overlapping areas. The proportion of overlap between the various images indicates that a majority of the tPA-induced synaptic connections accumulated recycled vesicles and were associated with clusters of GluR1 receptors.

L-LTP, we perfused purified tPA onto hippocampal slices. We first examined the mossy fiber–CA3 pathway and found that tPA (0.5 μg/ml) did not significantly alter the basal transmission level. However, when the application of tPA was paired with a single tetanus it induced sustained L-LTP (3 hr after the tetanus, +tPA 213% ± 8%, $n = 4$, control 118% ± 10%, $n = 4$, $p < 0.01$, tPA alone 117% ± 8%, $n = 4$, $p < 0.01$) (Figure 1E). Moreover, the facilitated induction of L-LTP by tPA was strongly depressed by the tPA inhibitor PAI-1 (1 μg/ml) (Figure 1E). Similarly, in the Schaffer collateral pathway, application of purified tPA protein for 20 min did not induce significant synaptic potentiation (Figure 1F). However, when the application of tPA was paired with a single tetanus, which normally only induces the early phase of LTP in the Schaffer collateral pathway, a sustained late phase of LTP emerged (Figure 1F). Three hours after pairing a single train with tPA, Schaffer pathway LTP increased to 180% ± 15% ($n = 5$), and after single tetanus alone it increased to 118% ± 4%, $n = 5$, $p < 0.01$ (Figure 1F). These results suggest that the extracellular activity of tPA is capable of contributing to the induction of L-LTP in both the mossy fiber and Schaffer collateral pathways.

Localization, Expression, and Release of tPA

Extracellular tPA activity has been found to increase in the hippocampus after membrane depolarization, probably as a result of being secreted (Gualandris et al., 1996). To determine whether tPA is expressed by neurons and whether it is secreted into the extracellular medium, we reconstituted the mossy fiber–CA3 synaptic connection in dissociated cell culture as previously described (Baranes et al., 1996). Using immunocytochemical analysis, we found that tPA is present in neuronal cell bodies (Figure 2a), where it is colocalized with MAP2 (Figure 2b). This is in agreement with studies describing the subcellular distribution of tPA in the cerebellum (Seeds et al., 1995). We were unable to determine whether tPA protein is present in axons and axonal varicosities. However, Griesinger and Schweizer (1997, Soc. Neurosci., abstract) have found that approximately 20% of presynaptic terminals of neurons cultured from total embryonic hippocampi are immunoreactive for tPA.

To measure mRNA expression and secretion of tPA from the entire cell population in the culture, we exposed the culture to forskolin. We did this for several reasons. First, as mentioned above, forskolin can induce both an early and a late phase of LTP in the mossy fiber pathway in hippocampal slices (Huang et al., 1994; Weisskopf et al., 1994). Second, forskolin produces a long-lasting potentiation of cultured neurons of the mossy fiber pathway (López-García et al., 1996). Third, the activation of the cAMP cascade alters the activity level of tPA in PC12 cells (Leprince et al., 1991). Finally, the tPA gene has a CRE region in its promoter (Ohlsson et al., 1993).

We found that stimulation of cultured granule and CA3 pyramidal neurons with forskolin triggered a rapid, Ca^{2+}-dependent secretion of tPA (Figures 2c and 2d). Release began several minutes after application of forskolin, plateaued at 37% ± 1.0% above control 5 min after application, and was inhibited by 89% ± 6% when extracellular Ca^{2+} was omitted. Secretion of tPA was also produced by Sp-cAMPs, suggesting that the effect of forskolin was due to stimulation of the cAMP pathway (Figure 2d). Forskolin also increased the level of tPA mRNA in these neurons (Figure 2e). Using Northern blot analysis, this increase was first detected 30 min after stimulation, reaching a 5-fold increase 3 hr poststimulation.

Forskolin Induces Varicosity Formation and Axonal Elongation

We next asked whether the application of forskolin to cultured cells is also accompanied by the remodeling of synaptic connections and, if so, whether tPA is involved in this structural plasticity. Toward this end, we developed specific protocols for stimulating and monitoring individual neuronal processes and their synaptic connections for periods of up to 2 weeks in duration. We labeled neurons in culture for up to 2 weeks with dissolved or crystallized DiI and found preferential labeling of axons and axonal varicosities. We next confirmed the labeling of axons and their varicosities using antibodies to the synaptic vesicle membrane protein synaptophysin and found that more than 80% of the DiI-labeled varicosity-like structures along neuronal processes were immunoreactive (Table 1, also see Figure 7).

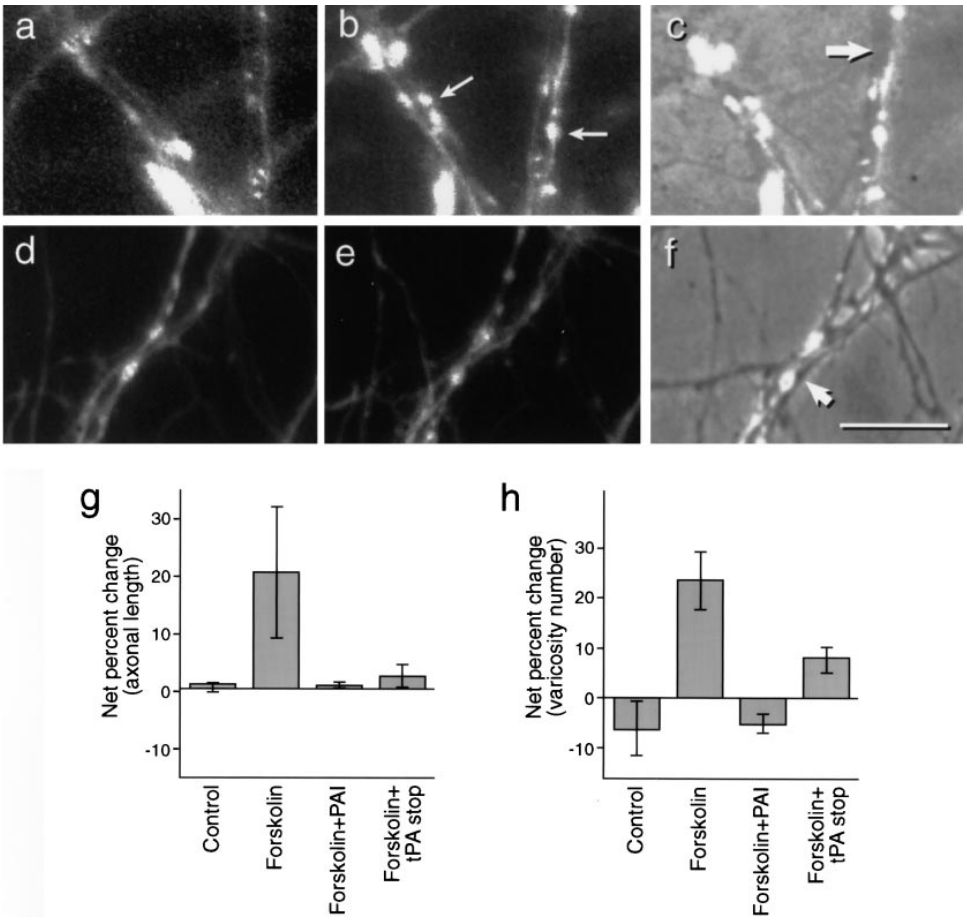

Figure 3. Forskolin-Induced Varicosity Formation and Axonal Elongation in the Presence and Absence of tPA Inhibitors

DiI-labeled axons of 12- to 15-day-old granule cells of the dentate gyrus were imaged before ([a], forskolin; [d], forskolin and PAI-1) and 6.5 hr following stimulation ([b], forskolin; [e], forskolin and PAI-1). (c and f) Same fields as (a) and (b), and (d) and (e), respectively, superimposed with the phase contrast image. Note the DiI-labeled processes are fasciculating with dendrites (indicated by the thick arrows in [c] and [f]). These processes run along the dendrites and express varicosities-like structures. In culture this appearance is unique for axons. The net increase in varicosity number after forskolin stimulation is 4 (two of the newly formed varicosities are indicated by small arrows in [b]) in the absence of PAI-1, and 0 in its presence. (a)–(c) are representative of 26 fields out of 16 dishes from 12 separate experiments. (d)–(f) represent 12 fields of six dishes from four separate experiments. Occasionally we found an increase in DiI labeling of axonal shafts probably as a result of the repetitive fluorescent illumination or changes in pH during the 10 hr experiments. This increase was observed in some but not all of the experiments and was similar in stimulated and control cells; therefore, it was ignored.

Total axonal length and the number of varicosities in each field were compared before (time 0) and 6.5 hr after the application of forskolin in the presence or absence of tPA inhibitors. The percent change $\pm$ standard error was plotted in (g) for axons and (h) for varicosities. The mean initial axonal length per field before treatment was 499.3 $\pm$ 58.9 μm for control and 557.2 $\pm$ 70.9 μm for the experimental group. The mean initial varicosity number per field was 35.4 $\pm$ 3.7 for control and 46.5 $\pm$ 7.3 for the experimental group. These differences were not statistically significant ($p > 0.5$). PAI-1, 12 fields out of six dishes from four experiments. tPA stop, four fields of two dishes from two experiments.

We next stimulated the cells pharmacologically using a blind procedure. We did so by presenting the pharmacological agent to the cells bathed in culture medium without a pre- or poststimulation wash. This was done to reduce cell toxicity and to maintain a low level of spontaneous process outgrowth. As the occurrence of morphological modifications was found to be on the order of hours, the stimulus was maintained for 6–10 hr.

Stimulation of labeled cells with forskolin resulted in the formation of varicosity-like swellings along axonal processes fasciculated with dendrites and at 6 hr reached a level of 24% $\pm$ 7% above that evident at time 0 ($n = 26$ fields in 12 experiments), whereas the level found in nonstimulated cells was $-7\% \pm 7\%$ ($n = 22$ fields in 10 experiments; $p < 0.05$) (Figures 3a, 3b, and 3h). This effect of forskolin was inhibited by both tPA inhibitors, PAI-1 and tPA stop (Figures 3d, 3e, and 3h) by 100% ($p < 0.05$; $n = 10$ fields from three experiments) and 62% $\pm$ 4%, respectively. The tPA inhibitors did not significantly affect the spontaneous level of varicosity formation in the absence of forskolin.

Forskolin stimulation also resulted in the elongation of axons. The extent of elongation 6 hr after stimulation was 21% $\pm$ 11% ($p < 0.03$) greater than time 0 (Figure 3g). Stimulation of cells with forskolin in the presence of PAI-1 or tPA stop also inhibited axonal elongation

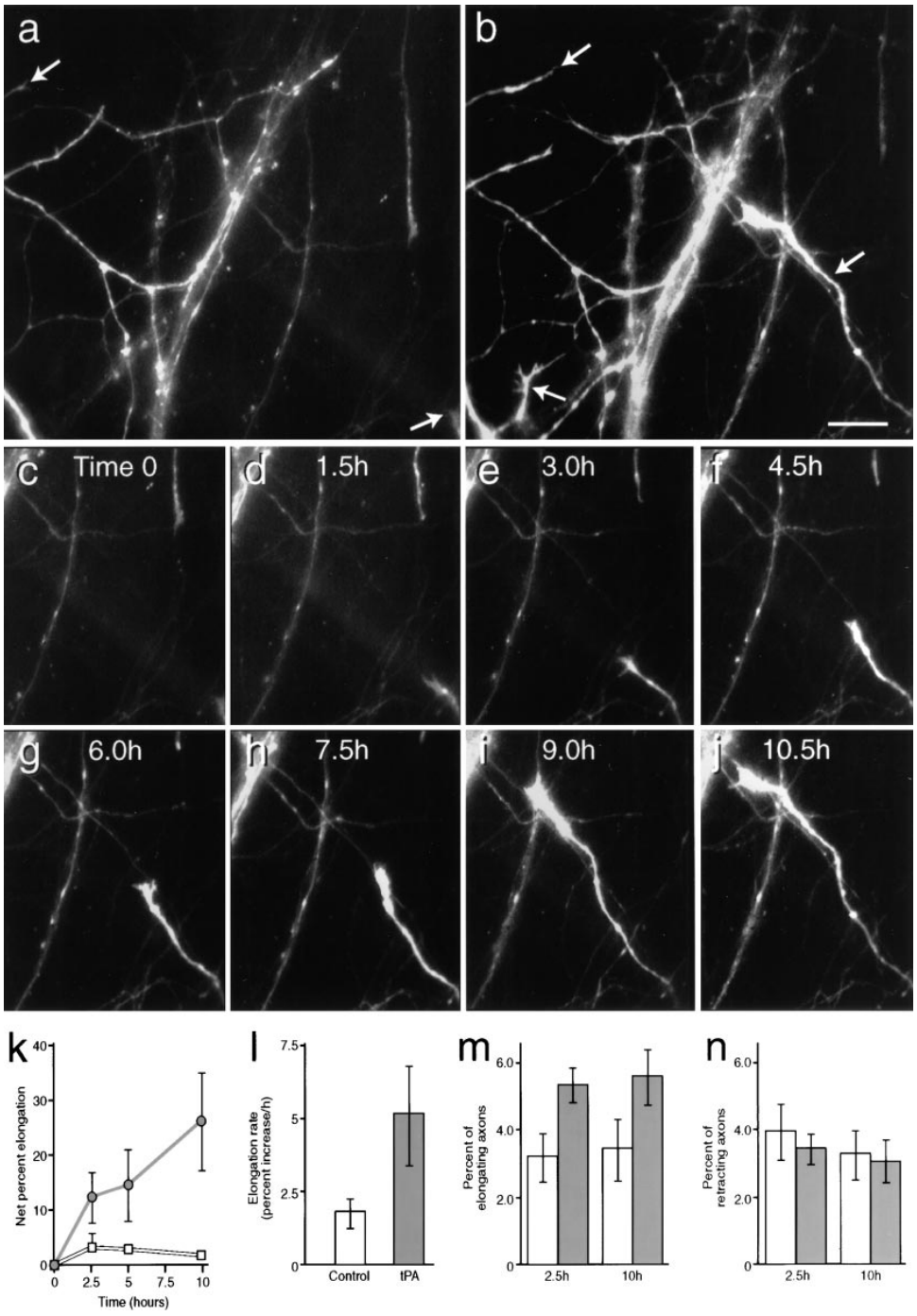

Figure 4. tPA-Induced Axonal Elongation

Dentate gyrus granule cells were selectively labeled with DiI for up to 15 days, then their axons were imaged (a) before and (b) 10 hr after exposure to tPA (b). Arrows indicate three processes that elongated after exposure to tPA. With the exception of the process in the lower left portion of the field (b), all of these were immunoreactive for the axonal marker NFM (data not shown). (c–j) Time lapse recording of the elongation of the axon indicated by an arrow at the lower right of (a). Shown is a representative field out of 18 fields from 11 separate stimulation experiments. Note that in the bottom center of (b) and (j) the new varicosities were formed on elongating axons. Scale bar, 10 μm.

(k) Kinetics of axonal elongation in response to tPA. The total length of DiI-labeled axons in each field was measured at different time points following stimulation by tPA or the control solution. The net percent of change relative to time 0 is plotted. Open squares, nonstimulated; filled circles, tPA stimulated.

(l) Rate of axonal elongation increased by tPA treatment. The vertical axis represents the percent increase in axonal length during each time interval. tPA increases the number of elongating axons (m) but did not affect the number of those axons retracting (n). Open boxes, nonstimulated; filled boxes, tPA stimulated. Axons were defined as elongating or retracting if they increased or decreased their length by more than 1 μm at a time interval compared to time 0. Each point on the graph is the percent of the number of elongating or retracting axons vs. total axonal number. The data for this analysis was gathered from 18 fields of stimulated cells from 11 experiments, and 16 fields from 9 control experiments.

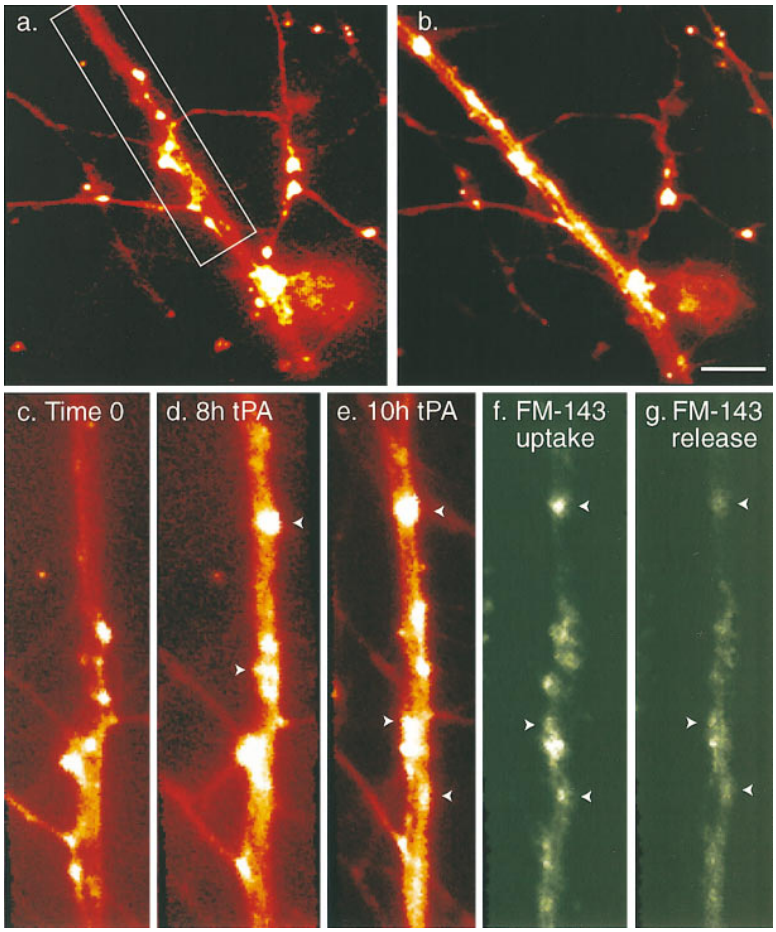

Figure 5. tPA Induces Formation of Axonal Varicosities Containing cAMP-Sensitive Secretory Machinery

The different DiI fluorescent intensities within axons and resident varicosities, presumably a result of different inherent volumes, were digitally enhanced. Axons appear reddish yellow, and varicosities appear white. (a) Time 0. (b) Same field as (a), 10 hr after exposure to tPA. (c–g) Magnification of the area boxed in (a). Arrowheads in (d) and (e) indicate regions of varicosity turnover. The net increase in number of varicosities between 10 hr tPA (e) and time 0 (c) is 2. Arrowheads in (f) and (g) indicate the uptake and release, respectively, of FM143 (white dots) at newly formed varicosities, following forskolin stimulation. Under these conditions the extent of release from newly formed and preexisting varicosities was similar, averaging ~70%. Scale bar for (a) and (b), 10 μm; (c)–(g), 7 μm.

(Figure 3g). These results suggest that tPA activity can contribute to forskolin-induced axonal elongation and synapse formation in the mossy fiber pathway.

tPA Induces Elongation of Mossy Fibers

Both axonal elongation and the production of new synaptic structures could be induced by tPA. The elongation of axons was more pronounced during extracellular application of purified double chain tPA (Figure 4) than that measured following forskolin stimulation. This effect was inhibited by PAI-1 (data not shown), indicating that it required the proteolytic activity of tPA. Elongation was first observed at 2.5 hr following tPA stimulation (Figure 4k) and increased with time at an average rate of 15 ± 5 μm/hr, a value 3-fold greater ($p < 0.03$) than the average rate of axonal elongation of nonstimulated cells (Figure 4l). Elongation reached a peak value of 126% ± 8.0% compared to the total axonal length at time 0 ($p < 0.03$), 10 hr after the triggering with tPA (Figure 4k). This increase in length was approximately 10-fold greater than the spontaneous elongation of axons of nonstimulated cells at the same time point. Quantitative analysis of the changes in length of individual axons revealed that the effect of tPA was via induction of elongation ($p < 0.05$) (Figure 4m) and not through inhibition of retraction ($p > 0.1$) (Figure 4n).

Axons of cells exposed to tPA elongated while fasciculating with dendrites or when extending on the glial monolayer toward a defined target on dendrites (data not shown). Only rarely did elongation occur in the absence of a postsynaptic target. We used phase contrast (data not shown) to verify that elongation resulted from extension of the axons and not from dye accumulation in unlabeled processes.

tPA Induces Formation of Active Presynaptic Varicosities

The application of extracellular tPA produced an increase in the number of axonal varicosities similar to that produced by forskolin stimulation (Figures 5, 7a, and 7b) with a maximal increase of 33% ± 5% at 10–11 hr after the onset of application compared to time 0 ($p < 0.009$) (Figures 5a–5e and 6a). This effect of tPA was blocked by PAI-1. Of the tPA-induced varicosities, 80% contained synaptic vesicles as detected by synaptophysin immunoreactivity (Figure 7 and Table 1), and 60%

The mean initial axonal length per field before treatment was 499.3 ± 58.9 for control and 557.2 ± 70.9 μm for the experimental group. The mean initial number of axons per field was 12 ± 3.2 for control and 13 ± 1.4 for the experimental group. These differences were not significant ($p > 0.5$).

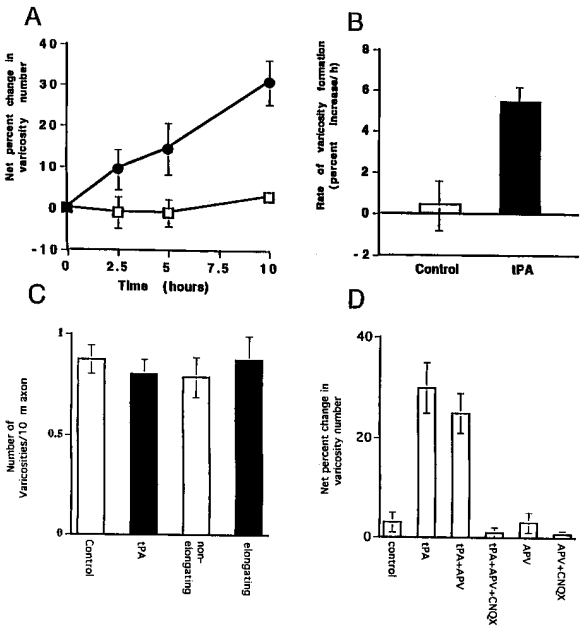

Figure 6. Quantification of tPA-Induced Varicosity Formation

(A) Kinetics of varicosity formation in response to tPA trigger. The total varicosity number in each field was measured at different time points after exposure to tPA or control solution. Each point represents the net percent change in number of varicosities relative to time 0. Filled circles, tPA stimulation; open squares, control.

(B) tPA increases the rate of varicosity formation compared to that measured in nonstimulated cells. Open bar, nonstimulated; filled bar, tPA stimulated. The mean initial varicosity number per field was 35.4 ± 3.7 for control and 46.5 ± 7.3 for the experimental group. These differences were not statistically significant ($p > 0.5$).

(C) Density of varicosities for the total population of axons, or specifically for extending axons, was not affected by tPA. At each time point the concentration was calculated by dividing the total number of varicosities by the total axonal length, or it was performed on nonelongating (open bars) and elongating (filled bars) axons separately. Shown is the mean ± SEM of 18 different fields out of 11 separate control and stimulation experiments.

(D) Effect of synaptic activity on varicosity formation. Cells were exposed to the inhibitors of glutamate receptors APV and CNQX in the presence or the absence of tPA. Eight hours after stimulation, the number of varicosities was calculated as mentioned above. Shown is the mean ± SEM of three experiments.

displayed the ability to recycle vesicles as they took up and secreted the styryl dye FM-143 following exposure to forskolin (Figures 5c–5g and Table 1), similar to recycling exhibited by preexisting varicosities (Table 1). These results demonstrate that in culture tPA increases, by approximately 20%, the number of functionally competent presynaptic release sites.

Similar to the kinetics of axonal elongation (Figure 4k), the increase in the number of varicosities began at approximately 2.5 hr following tPA stimulation (Figure 6a) and continued to increase at a rate of 5%/hr (Figure 6b), which was approximately 8-fold higher than the average rate found in nonstimulated cells ($p < 0.02$).

Since the increase in varicosities occurred with kinetics similar to those of axonal elongation (both 5%/hr), we also examined whether tPA stimulation produced any change in the final density of varicosities per unit length of axon. This proved not to be the case. tPA increased both axonal length and the number of varicosities in the same proportion at different time intervals, such that the final density of varicosities per axonal unit was not significantly different from the density measured at time 0 ($p > 0.3$) (Figure 6c). Moreover, the final concentration of varicosities on elongating axons was similar to that of nonelongating axons (Figure 6c). These results suggest the total number of varicosities per unit length of axon may be regulated.

However, although the length of axons increases, the length of dendrites remains approximately the same before and after stimulation. Forskolin and tPA actually increase the number of varicosities per dendrite (see Figures 3a–3c and Figure 5). This is in agreement with the findings of Bolshakov et al. (1997) who measured an increase in synaptic input following induction of hippocampal LTP.

As described above, we routinely included the NMDA receptor antagonist APV in our cultures. When CNQX, an inhibitor of glutamatergic AMPA receptors, was present during tPA stimulation in addition to APV, the effect of tPA on varicosity formation was blocked (from 25% ± 4% to 3% ± 1%, n = 3, Figure 6d). On the other hand, if CNQX and APV were both omitted during tPA stimulation, the effect of tPA on varicosity formation was slightly stronger than when APV was present alone (30% ± 5% vs. 25% ± 4%, n = 3). The effect of these inhibitors in the absence of tPA was not significantly different when compared to the level of varicosity formation in control, nonstimulated cells. These results indicate that active AMPA glutamate receptors are necessary for tPA-induced synaptic structural changes to occur. We obtained similar results using glutamate receptor blockers during forskolin stimulation (data not shown). Both the effects of forskolin on varicosity formation and on axonal elongation were blocked by exposure of the cells to TTX (n = 3, data not shown). This suggests that this form of synaptic structural plasticity requires synaptic activity. The inhibitory effect of APV may be related to the observation that synaptic transmission in the mossy fibers is at least partially mediated through an NMDA-sensitive component both in vitro (López-García et al., 1996) and in vivo (Jonas et al., 1993; Weisskopf and Nicoll, 1995). Therefore, it is likely that in the absence of APV there is a higher level of spontaneous activity contributing to an increase in synapse formation.

In our electrophysiological analysis, both application of tPA and electrical stimulation were required in order to induce L-LTP (see Figure 1). The results described here suggest that, perhaps in a similar way, the effect of tPA on varicosity formation is dependent on activity.

Postsynaptic Target of Varicosity Formation

The finding that tPA is blocked by inhibitors of glutamate receptors suggests that tPA may have a corresponding effect on the postsynaptic target of newly formed presynaptic varicosities. If so, does the formation of postsynaptic sites precede the formation of varicosities, or is the presence of the postsynaptic target required for presynaptic outgrowth? As can be seen in Figures 3, 5, and 7, formation of axonal varicosities occurred almost exclusively on axons that fasciculated with dendrites.

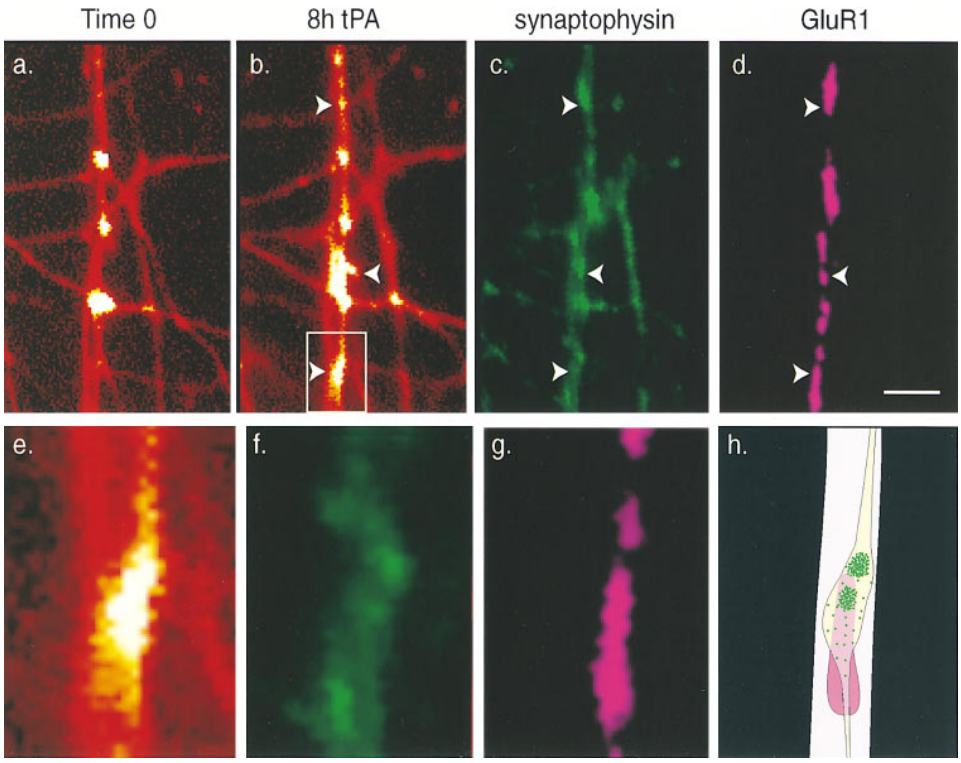

Figure 7. tPA-Dependent Formation of Axonal Varicosities Occurs Contiguous to Patches of GluR1 Receptors on Dendrites

Stimulated and control cells were fixed at the end of the experiment, the DiI fluorescence was bleached, and cells were immunolabeled with antibodies to synaptophysin and GluR1 receptors. Double-labeled images were superimposed to detect colocalization (data not shown). Varicosities in images (a), (b), and (e) are shown in white using digital enhancement as in Figure 5. (a) Time 0. (b) Same field as (a), 8 hr after exposure to tPA. Arrowheads indicate newly formed varicosities. All varicosities were formed on two central axons fasciculating with the dendritic process (the dendrites are shown in purple following GluR1 staining in [d]) and not on other nonfasciculating axons. (c) Same field as (a) stained with antibodies to synaptophysin. The arrowheads in (c) and (d) have identical locations in the field. Note that the newly formed varicosities are synaptophysin positive and overlap with dendritic clusters of GluR1. (e) Magnification of one newly formed varicosity in the boxed area of (a) and the corresponding synaptophysin (f) and GluR1 (g) images. These images were superimposed, and the percentage of overlap was expressed as a change in the original color. The diagram in (h) illustrates the resultant combination of individual images in (e), (f), and (g). The newly formed varicosity (yellow) and its two synaptic vesicle pools (green) overlap with a cluster of GluR1 receptors (purple). The analysis of these results is presented in Table 1. Scale for (a)–(d), 6.5 μm; (e)–(h), 1.8 μm.

Rarely did these appear in the absence of a postsynaptic process. Moreover, the pattern of varicosity formation was not random. Rather, it took place near clusters of GluR1 receptors on the dendrite (Figure 7 and Table 1). GluR1 receptors are expressed along the entire dendritic tree and occasionally appear as hot spots, two to three times more intense in fluorescence than the shaft (Figures 7d and 7g) (see Craig et al., 1993; Baranes et al., 1996). To assess the level of association between varicosity formation and GluR1 clusters, fluorescent images of processes labeled with DiI and double labeled with synaptophysin and GluR1 receptor antibodies were superimposed (Table 1 and Figures 7e–7h). We found 88% ± 11% of the tPA-induced varicosities occurred directly opposite GluR1 hot spots on dendrites (Figure 7 and Table 1), as was the case with greater than 80% of preexisting varicosities. Inclusion of only the newly formed varicosities that contained synaptic vesicles increased the colocalization to 95% ± 5%. Moreover, all of the newly formed varicosities containing releasable synaptic vesicles were in apposition to GluR1 patches. However, it is not clear to us whether GluR1 aggregation precedes varicosities formation or whether the opposite is the case. Thus, in culture, tPA appears capable of inducing the formation of functionally competent glutamatergic synapses consisting of an active, presynaptic secretory component and a postsynaptic recognition component enriched with glutamate receptors.

Discussion

The finding that tPA is upregulated during LTP (Qian et al., 1993) has encouraged us to test the specific hypothesis that this serine protease is importantly involved in the persistence of this form of hippocampal plasticity (Frey et al., 1996; Huang et al., 1996). We have focused on two types of plastic events: potentiation of synaptic strength (LTP) in hippocampal slices and enhancement of synapse formation in dissociated hippocampal cell culture. Using both purified tPA and specific inhibitors, we found that tPA is involved in L-LTP in the mossy fiber pathway in hippocampal slices, and that tPA produces axonal elongation of mossy fibers and promotes the formation of synaptic varicosities in hippocampal culture. We also demonstrate that in response to elevated

levels of cAMP endogenous tPA is first secreted and then acts extracellularly.

The findings that the extracellular activity of tPA can induce synaptic structural changes and enhance LTP induced by a single tetanic stimulation in the cells of the mossy fiber pathway, and that both effects are upregulated by synaptic activity, raise the possibility that these two plastic processes may be related. For example, the increase in cAMP following induction of LTP may lead to an increased expression of tPA and its subsequent release into the extracellular space. The idea that tPA is secreted in an activity-dependent manner from axons is supported by the recent demonstration that tPA is localized within presynaptic terminals of hippocampal cells in culture (Griesinger and Schweizer, 1997, Soc. Neurosci., abstract). Secreted tPA could, in turn, initiate axonal elongation and promote the formation of new active synaptic connections. Because patch recordings are relatively short lasting, we have not yet demonstrated that these slow structural changes directly affect synaptic activity in cell culture. Nevertheless, it is attractive to think that the increase in synapse number may account for at least a portion of the increase in synaptic efficacy associated with LTP.

Other serine proteases, such as thrombin, which has been reported to induce axonal retraction (Gurwitz and Cunningham, 1988; Monard, 1988; Brewer, 1995), may have related roles in structural plasticity. Thus, the release and activation of this class of proteases may be a general component of the mechanisms whereby activity-dependent synaptic modifications become stabilized by structural changes. In addition to serine proteases, other synaptogenic cues are probably involved, explaining the residual L-LTP found in the presence of tPA stop and in tPA knockout mice (Frey et al., 1996; Huang et al., 1996).

The finding that the expression of tPA in cells of the mossy fiber pathway can be induced by activation of the cAMP cascade is consistent with the fact that the tPA gene has a CRE region in its promoter (Ohlsson et al., 1993) and that CREB and other CRE binding proteins are involved in a variety of enduring forms of synaptic plasticity (Dash et al., 1990; Bourtchouladze et al., 1994; Bartschet al., 1995). Thus, in the molecular cascade that underlies learning-related plasticity in the mammalian brain, the expression of tPA mRNA may prove to be a critical effector downstream from CREB.

Varicosity Formation Is Targeted toward Dendritic Patches of GluR1 Receptors

Our results show that the formation of presynaptic varicosities occurs contiguous to specialized postsynaptic regions on dendrites that are enriched with GluR1 receptors. This is similar to what has been reported in sensory–motor neuron cocultures of *Aplysia* where the postsynaptic cell is required for induction of presynaptic varicosity formation (Glanzman et al., 1990). These findings suggest that the aggregation of GluR1 receptors evident as patches along dendrites, in apposition with tPA-induced presynaptic varicosities, may represent postsynaptic specializations.

It is not clear whether GluR1 aggregation precedes or is induced by synaptic activity. Since a portion of the GluR1 patches appear in association with growth cones and synaptic vesicle–depleted varicosities (Table 1), it is also possible that GluR1 clustering has a developmental role in synaptogenesis, perhaps resembling the aggregation of acetylcholine receptors during formation of the neuromuscular junction (Campanelli et al., 1991; Froehner, 1991). Regardless of the specific role that the clustering of GluR1 plays, our results suggest that tPA induces the formation of axo-dendritic structures which have the characteristics of functional glutamatergic synapses: they consist of a presynaptic site with releasable synaptic vesicles and a postsynaptic site enriched with glutamate receptors.

How might tPA mediate its action on LTP and axonal elongation and synaptogenesis? Since these actions of tPA were inhibited by PAI-1 and tPA stop, our results suggest that they were mediated through the catalytic domain of tPA (Figures 1 and 3). These actions could be accomplished in one of several ways. One, tPA could alter the adhesiveness of neurites to their extracellular environment, enabling them to grow. This could be achieved by the cleavage of adhesion molecules that are expressed by the cell or by the extracellular matrix, as has been suggested for fibronectin (Seeds et al., 1990). Alternatively, tPA could produce its action by activating a growth factor such as HGF. HGF is inactive in the basal state. But it can be activated through proteolytic cleavage mediated by tPA (Honda et al., 1995; Naldini et al., 1995; Thewke and Seeds, 1996). Once activated, HGF affects the survival of hippocampal neurons through its receptor, the c-Met tyrosine kinase (Honda et al., 1995; Naldini et al., 1995; Thewke and Seeds, 1996). In addition, HGF functions as a chemoattractant for axons of motor neurons (Ebens et al., 1996). Therefore, it is possible that tPA induces cleavage and activation of HGF, which then induces axonal elongation. tPA may act on the motility of the growth cone, since it is secreted from axonal tips (Pittman et al., 1989; Seeds et al., 1990). However, since tPA was also found in presynaptic terminals (Griesinger and Schweizer, 1997, Soc. Neurosci., abstract), this protease may have a highly localized role in synaptic growth, perhaps utilizing the same mechanisms underlying its action on axonal growth.

Axonal elongation and synapse formation by tPA could reveal a function of tPA unrelated to its proteolytic activity. For example, uPA, a reactive serine protease, prevents the binding of PAI-I to fibronectin, enabling integrin to bind and promote cellular migration, a function that does not involve the proteolytic activity of uPA (Stefansson and Lawrence, 1996). Also, tPA may directly produce intracellular signaling leading to structural modifications through its membrane binding site (Pittman et al., 1989; Verrall and Seeds, 1989).

How does tPA act on L-LTP? Our data suggest that tPA may be necessary but not sufficient for L-LTP. In addition to tPA, the maintenance of L-LTP requires weak synaptic activity (see Figures 1E and 1F). As shown in Figure 6d, activity coincident with the application of tPA produces a maximal effect on synapse number similar to what we report is required to produce L-LTP with tPA. Thus, although tPA alone produces some level of

synaptic structural change, we suggest that tPA activity has to coincide with synaptic activity to achieve the full degree of synapse formation that is required to maintain LTP.

That these mechanisms can be recruited by fully differentiated neurons suggests that learning-related synaptic plasticity initiated by experience in the adult brain may share a common molecular logic with the refinement of synaptic connections that shapes the developing nervous system.

Experimental Procedures

Electrophysiology

Sprague-Dawley rats (5- to 6-weeks old) were decapitated, and their brains were quickly removed into oxygenated iced artificial cerebral spinal fluid (ACSF). Transverse hippocampal slices (400 μM) were prepared and placed in an interface slice chamber at a constant temperature of 28°C. The slices were perfused with ACSF solution containing 124 mM NaCl, 1.3 mM $MgSO_4$, 4 mM KCl, 1.0 mM Na_2HPO_4, 2.0 mM $CaCl_2$, 26 mM $NaHCO_3$, and 10 mM D-glucose, at 2.0 ml/min. In some experiments, slices were perfused with ACSF solution containing picrotoxin (20 μM; the $MgSO_4$ and $CaCl_2$ in these ACSF solutions were 4 mM). Stainless steel electrodes were used for long-lasting extracellular recording, and a fine tungsten bipolar steel electrode was used to elicit the synaptic response. To record the excitatory postsynaptic potential from the mossy fiber pathway, the stimulating electrode was placed in the granule cell layer, and the recording electrode was placed in the stratum lucidum of the CA3 region. In each experiment, the positions of both the stimulating and recording electrodes were adjusted until the excitatory postsynaptic potential (EPSP) recorded met criteria described previously (Zalutsky and Nicoll, 1990). Moreover, 25 μM APV was used in all LTP experiments to block possible contamination from the NMDA-dependent commissural pathway. To record the EPSP in the CA1 region, the stimulating electrode was placed in CA3 Schaffer collateral commissural fibers. Test stimuli were of 0.05 ms pulse duration and 0.016 Hz frequency. LTP was elicited with one or three trains (100 Hz for 1 s; the pulse duration was 0.1 ms, which was twice that of the test stimuli). The EPSP was measured as slope (mV/ms), and LTP was plotted as percentage change of baseline EPSP slope.

For bath application, the following drugs were made and stored as concentrated stock solutions and then diluted 1000-fold when applied to the perfusion solution: 25 mM APV (±2-amino-5-phosphonopenanoic acid, RBI), 50 mM forskolin (RBI, dissolved in DMSO); 2 mM synthetic tPA inhibitor–tPA stop (America Diagnostica Inc. #544). For the application of tPA protein, the powder of two-chain tPA protein (standard, carrier free American Diagnostica Inc. #114) was directly dissolved in perfusion solution into a concentration of 0.5 μg/ml. tPA inhibitor PAI-1 (recombinase active mutant human PAI-1; America Diagnostica Inc. #1094) was applied to the perfusion solution at a concentration of 1 μg/ml.

Cell Culture

Hippocampi of P1-P4 rat pups were split longitudinally along the midportion of the CA3 region (see Baranes et al., 1996). Tissue containing part of the CA3 region and the entire dentate was treated for 30 min at 37°C with 0.25% trypsin (Sigma, type XI) and then gently triturated, and the dissociated cells were plated at a concentration of 2×10^5 ml onto poly-D-lysine (Sigma, 0.1 mg/ml) and laminin (Collaborative research, 10 μg/ml) coated glass coverslips.

Cells were plated in minimal essential medium Eagle (MEM; Sigma) containing 10% heat-inactivated fetal bovine serum (Hyclone), 2 mM glutamine, and 0.76% glucose. On the following day, the medium was replaced with fresh serum-free SF1C medium (Rayport et al., 1992), including B27 supplements (GIBCO). The cells were grown in a humid incubator, containing 5% CO_2 at 37°C, and the medium was not replaced during the entire culture period. The neurons survived in vitro for up to 12 weeks. Under these conditions, the ratio of dentate gyrus neurons to CA3 pyramidal neurons was higher than 10.

Immunocytochemistry

Cells were immunolabeled as described by Craig et al. (1993). The mouse antibodies used in this study were as follows: monoclonal anti-MAP2 (Sigma, 1 μg/ml); monoclonal antiSynaptophysin (Boehringer, 5 μg/ml). The rat antibodies were anti-GluR1 (Chemicon, 5 μg/ml) and anti-tPA (American Diagnostica, 10 μg/ml). tPA specificity was verified by competing the immunoreactivity of anti-tPA in the presence of excess tPA. The secondary antibodies were goat anti-rabbit or goat anti-mouse IgG conjugated to FITC or Cy3 (Jackson's lab). Cells were examined with an Axiovert100 Zeiss fluorescent microscope with green filter set for FITC and Texas red filter for Cy3. Photomicrographs were taken using a MC80 Zeiss camera and a Hamamatsu C2400 SIT camera.

Secretion and mRNA Expression of tPA

Cells were grown in 96-well dishes for 2 weeks and were then stimulated by 50 μM of a water-soluble derivative of forskolin (RBI #F-111) in Tyrodes buffer (containing in mM: NaCl 119, KCL 5, $MgCl_2$, glucose 30, HEPES 20 [pH 7.3], adjusted with sucrose to 330 mOsm/l), in the presence or absence of 4 mM Ca^{2+}. When Ca^{2+} was absent, 2 mM EDTA was included. The supernatant was collected at different time intervals, and tPA concentration was measured by ELISA, using the same antibody as for immunocytochemistry. The same purified tPA used for electrophysiological studies (see Electrophysiology) was used here as standard for quantitation.

For measuring mRNA expression, cells were treated with forskolin or control solution, total RNA was isolated using RNAzolB (Biotex Laboratories Inc.), and the expression was detected using Northern blot analysis.

Fluorescent Membrane Labeling and Cell Imaging

To selectively label mossy fibers, the dentate gyrus was anatomically separated from the CA3 region. After trituration, dentate gyrus cells were incubated for 1 hr with 100 μg/ml DiI (stock in Ethanol) in culture medium at 37°C. Cells were washed of dye residues by sedimentation through 5% bovine serum albumin in phosphate buffer saline. The pellet was rinsed with unlabeled CA3 cells at a ratio of 1:1 up to 10:1 DG:CA3. Cells were plated at a concentration of 2×10^5 cells/ml. The DiI labeled both axons and dendrites in culture. After 7–10 days in culture, DiI was internalized by the dendrites and retrogradely transported to the cell bodies. Axons (neurofilament M/[NFM] positive, data not shown), on the other hand, retained the dye for longer duration, enabling us to observe specifically fluorescent axons in 2-week-old cultures. This was confirmed by the finding that the DiI-positive varicosity-like swellings along labeled processes were immunoreactive for synaptophysin antibody and take up FM143.

In another set of experiments crystals of DiI were applied directly to the cells, which were originally plated at a high granule to pyramidal cell ratio, and recordings were performed 2–3 days later on labeled axons fasciculating with pyramidal dendrites. Under these conditions, the ratio between DiI-labeled mossy fiber and labeled axons of CA3 cells varied between 13:1 to 25:1, respectively.

Stimulation and Quantitation of Structural Changes

Analysis was based on the following restricted criteria: (a) For axonal elongation, an area was selected when it showed clear DiI-labeled processes (1–2 μm width) with varicosities and at least one growth cone. A varicosity was defined as a discrete expansion of fluorescence on a DiI-labeled process that had a round or oval shape and a diameter between 1–3 μm (Baranes et al., 1996). In some cases, as shown in Figures 7 and 9, the appearance of varicosities was verified using the styryl dye FM143 (see below) or antibodies to synaptophysin.

The empirical definition of nonelongating axons in our conditions was not absolute. Although we could observe and measure the elongation of axons by following the extension of their endings, we considered those that extended completely across the field as nonelongating when in fact they might have done so but out of the field. (b) For varicosity formation we chose an area showing one or

two DiI-labeled axons with varicosities fasciculating on an apical dendrite of pyramidal cells.

After an experimenter recorded a base line of 1–3 hr, a second experimenter applied the stimulation and control solutions as follows: water-soluble forskolin was applied at 50 μM with 50 μM of 3-Isobutyl-1-methylaxanthine (IBMX) in DMSO. Control culture received only DMSO (dilute × 100). To inhibit tPA activity, this enzyme was incubated for 10 min at room temperature with 2 μg of PAI-1 or tPA stop (1 μM), prior to stimulation (2 μg/500 μl/dish). When forskolin was used, the tPA inhibitors were introduced to the cells 10 min before stimulation. Mouse tPA double chain (see Electrophysiology) was used at a concentration of 1 μg/ml. All stimuli were performed in the culture medium in the presence of 50 μM APV. Control solutions contained everything in the stock solutions except the stimulator. In another set of experiments, APV was omitted during stimulation, or cells were stimulated in the presence of a mixture of APV and 6-cyano-7-nitroquinoxaline-2,3-dione (CNQX) (3 μM) or CNQX alone.

This was followed by time lapse recordings performed blindly by the first observer. Two other experimenters who did not know the history of the micrographs analyzed length of axons and number of varicosities. Exposure to forskolin or tPA for a period up to 48 hr did not produce any obvious cytotoxic effects. Since the spontaneous structural changes in control cells were high at this time point, we applied forskolin for up to 6 hr and tPA for up to 10 hr, exposure times during which the cultures were stable.

Image Recording and Processing

Images were taken on a Zeiss Axiovert 100 inverted microscope with a SIT (Hamamatsu C2400) video camera. The images were processed by Dell 310 computer with a PC vision Plus frame grabber and subsequently stored on a Storage Dimension optical disk drive.

Assessments of structural changes in these experiments were subject to potential artifacts resulting from differences in the amount of illumination light or differences in focal plane. Therefore, the experimenter always used the minimum intensity of illumination necessary to clearly visualize a cell's processes. Final images were composed of superimposed fluorescent images from two different focal planes that covered the entire process thickness. The first was taken from the bottom of the dish, where the glial monolayer lies and the next taken 3–5 microns above. A chroma 510-525 BP filter for FM-143 and a 590-610 BP filter for DiI were used.

Imaging of Synaptic Vesicle Recycling with the Styryl Dye FM-143

Following the last time lapse recording of a DiI-labeled field, the culture medium was replaced by Tyrode's buffer by slow perfusion (100–200 μl/min). FM143 (Molecular Probes) (15 μM) was applied for 1 min together with 50 μM forskolin. After 3 min washing with Tyrode's buffer, an image was recorded using 590-610 BP filter. The corresponding image of DiI overlapping at this range of wavelength was collected before the dye application and was subtracted from the FM-143 uptake image. Then forskolin was applied for 3 min in the absence of FM-143, and an image was recorded. Here again the corresponding DiI image obtained from the green filter was subtracted. The cells were then fixed with 4% paraformaldehyde and processed for immunocytochemistry.

Analysis of Data

All data are represented as the mean percent change ± SEM. The statistical analysis was by Student's t test.

Acknowledgments

We thank Dr. Tim Kennedy for his comments on the manuscript. We thank Mr. Jurek Karle and Mr. Konrad Kondratowicz for help in image processing and computer analysis, and Mr. Juan Carlos López-García for help in preparation of cell cultures. We also thank Harriet Ayers for typing the manuscript. This research was supported by the Howard Hughes Medical Institute (E. R. K.) and National Institutes of Health Grants MH37134 and GM32099 to C. H. B.

Received February 13, 1998; revised July 31, 1998.

References

Bailey, C.H., and Chen, M. (1988). Long-term memory in *Aplysia* modulates the total number of varicosities of single identified sensory neurons. Proc. Natl. Acad. Sci. USA *85*, 2373–2377.

Bailey, C.H., and Chen, M. (1989). Time course of structural changes at identified sensory neuron synapses during long-term sensitization in *Aplysia*. J. Neurosci. *9*, 1774–1780.

Bailey, C.H., and Kandel, E.R. (1993). Structural changes accompanying memory storage. Annu. Rev. Physiol. *55*, 397–426.

Bailey, C.H., Montarolo, P.G., Chen, M., Kandel, E.R., and Schacher, S. (1992). Inhibitors of protein and RNA synthesis block structural changes that accompany long-term heterosynaptic plasticity in *Aplysia*. Neuron *9*, 749–758.

Bartsch, D., Ghirardi, M., Skehel, P.A., Karl, K.A., Herder, S.P., Chen, M., Bailey, C.H., and Kandel, E.R. (1995). *Aplysia* CREB2 represses long-term facilitation: relief of repression converts transient facilitation into long-term functional and structural change. Cell *83*, 979–992.

Baranes, D., López-García, J.C., Chen, M., Bailey, C.H., and Kandel, E.R. (1996). Reconstitution of the hippocampal mossy fiber and associational-commissural pathways in a novel dissociated cell culture system. Proc. Natl. Acad. Sci. USA *93*, 4706–4711.

Bolshakov, V.Y., Golan, H., Kandel, E.R., and Siegelbaum, S. (1997) Recruitment of new sites of release during the cAMP-dependent late phase of long-term potentiation at CA3-CA1 synapses in the hippocampus. Neuron *19*, 635–651.

Bottaro, D.P., Rubin, J.S., Faletto, D.L., Chan, A.M.L., Kmiecick, T.E., Vande Woude, G.F., and Aaronson, S.A. (1991). Identification of the hepatocyte growth factor receptor as the c-met proto-oncogene. Science *251*, 802–804.

Bourtchouladze, R., Frenguelli, B., Cioffi, D., Blendy, J., Schutz, G., and Silva, A.J. (1994). Deficient long-term memory in mice with a targeted mutation of the cAMP responsive element binding (CREB) protein. Cell *79*, 59–68.

Brewer, G.J. (1995). Exogenous thrombin inhibits neuritogenesis in cultured neuroblastoma cells but not in rat hippocampal cells. Brain Res. *683*, 258–263.

Campanelli, J.T., Hoch, W., Rupp, F., Kreiner, T., and Scheller, R.H. (1991). Agrin mediates cell contact-induced acetylcholine receptor clustering. Cell *67*, 909–916.

Chang, F.-L.F., and Greenough, W.T. (1984). Transient and enduring morphological correlates of synaptic activity and efficacy change in the rat hippocampal slice. Brain Res. *309*, 35–46.

Craig, A.M., Blackstone, C.D., Huganir, R.I., and Banker, G. (1993). The distribution of glutamate receptors in cultured rat hippocampal neurons: postsynaptic clustering of AMPA-selective subunits. Neuron *10*, 1055–1068.

Dash, P.K., Hochner, B., and Kandel, E.R. (1990). Injection of the cAMP-responsive element into the nucleus of *Aplysia* sensory neurons blocks long-term facilitation. Nature *345*, 718–721.

Ebens, A., Brose, K., Leonardo, D.E., Hanson, G.M., Bladt, F. Jr., Birchmeier, C., Barres, B.A., and Tessier-Lavigne, M. (1996). Hepatocyte growth factor/scatter factor is an axonal chemoattractant and a neurotrophic factor for spinal motor neurons. Neuron *17*, 1157–1172.

Frey, U., Muller, M., and Kuhl, D.A. (1996). Different form of long-lasting potentiation revealed in tissue plasminogen activator mutant mice. J. Neurosci. *16*, 2057–2063.

Froehner, S.C. (1991). The submembrane machinery for nicotinic acetylcholine receptor clustering. J. Cell Biol. *114*, 1–7.

Geinisman, Y., de Toledo-Morrell, L., and Morrel, F. (1991). Induction of long-term potentiation is associated with an increase in the number of axospinous synapses with segmented postsynaptic densities. Brain Res. *566*, 77–88.

Geinisman, Y., de Toledo-Morrell, L., Morrel, F., Heller, R.E., Rossi, M., and Parshall, R.F. (1993). Structural synaptic correlates of long-term potentiation: formation of axospinous synapses with multiple, completely partitioned transmission zones. Hippocampus *3*, 435–446.

Glanzman, D.L., Kandel, E.R., and Schacher, S. (1990). Target-

dependent structural changes accompanying long-term synaptic facilitation in *Aplysia* neurons. Science *249*, 799–802.

Gualandris, A., Jones, T.E., Strickland, S., and Triska, S.E. (1996). Membrane depolarization induces calcium-dependent secretion of tissue plasminogen activator. J. Neurosci. *16*, 2220–2225.

Gurwitz, D., and Cunningham, D.D. (1988). Thrombin modulates and reverses neuroblastoma neurite outgrowth. Proc. Natl. Acad. Sci. USA *85*, 3440–3444.

Honda, S., Kagoshima, M., Wanaka, A., Tohyama, M., Matsumoto, K., and Nakamura, T. (1995). Localization and functional coupling of HGF and c-Met/HGF receptor in rat brain: implication as neurotrophic factor. Brain Res. Mol. Brain Res. *32*, 197–210.

Huang, Y.-Y., and Kandel, E.R. (1994). Recruitment of long-lasting and protein kinase A-dependent long-term potentiation in the CA1 region of hippocampus requires repeated tetanization. Learning Memory *1*, 74–82.

Huang, Y.-Y., Li, X.-C., and Kandel, E.R. (1994). cAMP contributes to mossy fiber LTP by initiating both a covalently-mediated early phase and macromolecular synthesis-dependent late phase. Cell *79*, 69–79.

Huang, Y.-Y., Bach, M.E., Lipp, H.-P., Zhuo, M., Wolfer, D.P., Hawkins, R.D., Schoonjians, L., Kandel, E.R., Godfraind, J.-M., Mulligan, R., Collen, D., and Carmeliet, P. (1996). Mice lacking the gene encoding tissue-type plasminogen activator show a selective interference with late-phase long-term potentiation in both Schaffer collateral and mossy fiber pathways. Proc. Natl. Acad. Sci. USA *93*, 8699–8704.

Jonas, P., Major, G., and Sakmann, B. (1993). Quantal components of unitary EPSCs at the mossy fiber synapse on CA3 pyramidal cells of rat hippocampus. J. Physiol. *472*, 615–663.

Lee, K., Schottler, F., Oliver, M., and Lynch, G. (1980). Brief bursts of high-frequency stimulation produce two types of structural change in rat hippocampus. J. Neurophysiol. *4*, 247–258.

Leprince, P., Rogister, B., Delrée, P., Rigo, J.M., André, B., and Moonen, G. (1991). Modulation of proteolytic activity during neuritogenesis in the PC12 nerve cells: differential control of plasminogen activator and plasminogen activator inhibitor activities by nerve growth factor and dibutyryl-cyclic AMP. J. Neurochem. *57*, 665–674.

López-García, J.C., Arancio, O., Kandel, E.R., and Baranes, D.A. (1996). A presynaptic locus for long-term potentiation of elementary synaptic transmission at mossy fiber synapses in culture. Proc. Natl. Acad. Sci. USA *93*, 4712–4717.

Mayer, M. (1990). Biochemical and biological aspects of the plasminogen activation system. Clin. Biochem. *23*, 197–211.

Monard, D. (1988). Cell-derived proteases and protease inhibitors as regulators of neurite outgrowth. Trends Neurosci. *11*, 541–544.

Naldini, L., Vigna, E., Bardelli, A., Follenzi, A., Galini, F., and Comoglio, P.M. (1995). Biological activation of pro-HGF (hepatocyte growth factor) by urokinase is controlled by a stoichiometric reaction. J. Biol. Chem. *270*, 603–611.

Nguyen, P.V., Abel, T., and Kandel, E.R. (1994). Requirement of a critical period of transcription for induction of a late phase of LTP. Science *265*, 1104–1107.

Nitecka, L., Tremblay, E., Charton, G., Bouillot, J.P., Berges, M., and Ben-Ari, Y. (1984). Maturation of kainic acid seizure-brain damage syndrome in the rat: II. histopathological sequelae. Neuroscience *13*, 1073–1094.

Ohlsson, M., Leonardsson, G., Jia, X.C., Feng, P., and Ny, T. (1993). Transcriptional regulation of the rat tissue type plasminogen activator gene: localization of DNA elements and nuclear factors mediating constitutive and cyclic AMP-induced expression. Mol. Cell. Biol. *13*, 266–275.

Okazaki, M.M., and Nadler, J.V. (1988). Protective effects of mossy fiber lesions against kainic acid-induced seizures and neuronal degeneration. Neuroscience *26*, 763–781.

Pittman, R.N., Ivins, J.K., and Buettner, H.M. (1989). Neuronal plasminogen activators: cell surface binding sites and involvement in neurite outgrowth. J. Neurosci. *9*, 4269–4286.

Qian, Z., Gilbert, M.E., Colicos, M., Kandel, E.R., and Kuhl, D. (1993). Tissue-plasminogen activator is induced as an immediate-early gene during seizure, kindling and long-term potentiation. Nature *361*, 453–457.

Rayport, S., Sulzer, D., Shi, W.X., Sawasdikosol, S., Monaco, J., Baston, D., and Rajendran, G. (1992). Identified postnatal mesolimbic dopamine neurons in culture: morphology and electrophysiology. J. Neurosci. *12*, 4264–4280.

Rickles, R.J., Darrow, A.L., and Strickland, S. (1988). Molecular cloning of complementary DNA to mouse tissue plasminogen activator mRNA and its expression during F9 teratocarcinoma cell differentiation. J. Biol. Chem. *263*, 1563–1569.

Rosen, E.M., Nigam, S.K., and Goldberg, I.D. (1994). Scatter factor and the c-met receptor: a paradigm for mesenchymal/epithelial interaction. J. Cell Biol. *127*, 1783–1787.

Seeds, N.W., Verrall, S., McGuire, P., and Friedmann, G. (1990). Plasminogen activator in the developing nervous system. In Serine Proteases and Their Serpin Inhibitors in the Nervous System, B.W. Festoff, ed. (New York: Plenum Press), pp. 173–184.

Seeds, N.W., Williams, B.L., and Bickford, P.C. (1995). Tissue plasminogen activator induction in Purkinje neurons after cerebellar motor learning. Science *270*, 1992–1994.

Sorra, K.E., and Harris, K.M. (1998). Stability in synapse number and size at 2hr after long-term potentiation in hippocampal area CA1. J. Neurosci. *15*, 658–671.

Stefansson, S., and Lawrence, D.A. (1996). The serpin PAI-1 inhibits cell migration by blocking integrin alpha V beta 3 binding to vitronectin. Nature *383*, 441–443.

Sumi, Y., Dent, M.A.R., Owen, D.E., Seeley, P.J., and Morris, R.J. (1992). The expression of tissue and urokinase-type plasminogen activators in neural development suggests different modes of proteolytic involvement in neuronal growth. Development *116*, 625–637.

Tauck, D.L., and Nadler, J.V. (1985). Evidence of functional mossy fiber sprouting in hippocampal formation of kainic acid-treated rats. J. Neurosci. *5*, 1016–1022.

Thewke, D.P., and Seeds, N.W. (1996). Expression of hepatocyte growth factor/scatter factor, its receptor, c-met, and tissue-type plasminogen activator during development of the murine olfactory system. J. Neurosci. *16*, 6933–6944.

Tsirka, S.E., Rogove, A.D., and Strickland, S. (1996). Neuronal cell death and tPA. Nature *384*, 123–134.

Tsirka, S.E., Rogove, A.D., Bugge, T.H., Degen, J.L., and Strickland, S. (1997). An extracellular proteolytic cascade promotes neuronal degeneration in the mouse hippocampus. J. Neurosci. *17*, 543–552.

Verrall, S., and Seeds, N.W. (1989). Characterization of ^{125}I-tissue plasminogen activator binding to cerebellar granule neurons. J. Cell Biol. *109*, 265–271.

Weisskopf, M.G., and Nicoll, R.A. (1995). Presynaptic changes during mossy fiber LTP revealed by NMDA receptor-mediated synaptic responses. Nature *376*, 256–259.

Weisskopf, M.G., Castillo, P.E., Zalutsky, R.A., and Nicoll, R.A. (1994). Mediation of hippocampal mossy fiber long-term potentiation by cyclic AMP. Science *265*, 1878–1882.

Zalutsky, R.A., and Nicoll, R.A. (1990). Mossy fiber long-term potentiation shows specificity but no apparent cooperativity. Neurosci. Lett. *138*, 193–197.